Chapter

Seismic Velocity Structure in and around the Japanese Island Arc Derived from Seismic Tomography Including NIED MOWLAS Hi-net and S-net Data

Makoto Matsubara, Hiroshi Sato, Kenji Uehira, Masashi Mochizuki, Toshihiko Kanazawa, Narumi Takahashi, Kensuke Suzuki and Shin'ichiro Kamiya

Abstract

Japanese Islands are composed of four plates, with two oceanic plates subducting beneath the two continental plates. In 2016 the National Research Institute for Earth Science and Disaster Resilience (NIED) Seafloor Observation Network for Earthquakes and Tsunamis along the Japan Trench (S-net) started seismic observation of the offshore Hokkaido to Boso region in the Pacific Ocean, and Dense Oceanfloor Network System for Earthquakes and Tsunamis (DONET) was transferred to NIED. We add the NIED S-net and DONET datasets to NIED high-sensitivity seismograph network (Hi-net) and full range seismograph network (F-net) datasets used in the previous study and obtain the three-dimensional seismic velocity structure beneath the Pacific Ocean as well as Japanese Islands. NIED S-net data dramatically improve the resolution beneath the Pacific Ocean at depths of 10–20 km because the seismic stations are located above the earthquakes and on the east side of the Japan Trench. We find a NS high-Vp zone at depths of 20–30 km. The 2018 Eastern Iburi earthquake occurred below the northern part of this high-V zone. The coseismic slip plane of the 2011 Tohoku-oki earthquake has low Vp/Vs, but its large slip region has high Vp. The broad low-Vp/Vs region may play a role in large earthquake occurrence.

Keywords: seismic tomography, failed rift, offshore event, NIED S-net, DONET, NIED Hi-net

1. Introduction

The Japanese Islands are mainly composed of the Eurasian (EUR) and the North American (NA) plates, and a number of small islands are on the Philippine Sea (PHS) and the Pacific (PAC) plates (**Figure 1**). The PHS and PAC oceanic plates are subducting beneath the EUR and the NA plates. A number of earthquakes occurred both at the plate interfaces and within the plates.

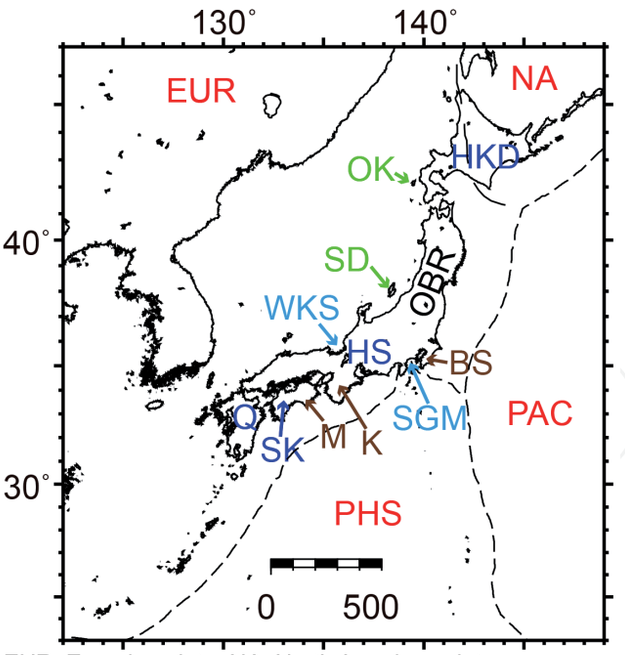

Figure 1.
Name of plates and location.

After the Kobe earthquake in January 1995, the Japanese government enacted the Special Measure Law on Earthquake Disaster Prevention in July 1995. This was to promote a comprehensive national policy on earthquake disaster prevention. Based on this goal, the National Research Institute for Earth Science and Disaster Resilience (NIED) contracted the deployment of the nationwide high-sensitivity seismograph network (Hi-net) [1] since NIED had already accumulated the experience for the Tokyo metropolitan deep borehole array and operated the Kanto-Tokai seismic network since 1979. NIED operates the Hi-net with approximately 800 stations since 2000 [2] and the full range seismograph network (F-net) [3] with approximately 70 stations composed of broadband seismographs since 1994 [4]. The Japan Meteorological Agency (JMA), the national universities, and other institutes operate other seismic networks with a total of approximately 600 stations for the detection of microseismicity. NIED operates ocean-bottom seismic stations beneath the Sagami Bay, while the JMA operates offshore the Tokai and Boso regions. The Earthquake Research Institute, University of Tokyo, operates the network offshore Sanriku, and the Japan Agency for Marine-Earth Science and Technology (JAMSTEC) operates offshore Kushiro and Muroto networks. JAMSTEC started the construction of the Dense Oceanfloor Network System for Earthquakes and Tsunamis (DONET) [5] off Kii and Muroto Peninsulas near the Nankai Trough in 2010, and they started operation networks offshore Kii (in 2014) and Muroto (in 2016) Peninsulas. NIED deployed the Seafloor Observation Network for Earthquakes and Tsunamis along the Japan Trench (S-net) [6] after the 2011 offshore Tohoku Earthquake (the Tohoku-oki event), which began operating in 2016 [7, 8]. DONET was transferred to NIED from April 2016. NIED started the operation of Monitoring of Waves on Land and Seafloor (MOWLAS) composed of Hi-net, F-net, S-net, DONET, strong-motion seismograph networks (K-NET and KiK-net) [9], and Volcano Observation Network (V-net) [10].

NIED S-net and DONET teams manually pick the arrival time data at the oceanic seismic stations after NIED Hi-net team has determined the hypocenters using the land stations. We confirm the difference of shallow hypocenters between the determination by only NIED Hi-net and that by NIED Hi-net and NIED S-net. Stars in **Figure 2** show the hypocenters at depths shallower than 20 km beneath the PAC plate determined by NIED Hi-net from September 11, 2017, to the end of 2018. The shallow hypocenters near the main island tend to remain shallow; however, hypocenters more than 200 km off the coast shifted significantly deeper to 40–80 km depth when including the S-net arrival time data (**Figure 2**). Deep events determined by NIED Hi-net on the east side of a longitude of 144°E are also shifted shallower. This suggests that it is important to include the S-net data for reliable hypocenter locations of offshore events.

Three-dimensional (3D) seismic velocity structure beneath the whole Japanese Islands has been studied using the vast data of seismic stations within the Japanese Islands maintained by NIED, JMA, national universities, and the other national and local governmental institutes (e.g., [11–14]). These studies used data obtained mainly at land-based seismic stations with a very few seismic stations on the sea floor such as Sagami Bay, off Kushiro, Sanriku, Boso, and Tokai regions. Reference [14] investigated the structure beneath the PAC plate at depths of 30–50 km using events that occurred under the Pacific Ocean (PO) with focal depths determined by NIED F-net. However, that study was not able to clarify the shallow structure beneath the PO at depths of 0–20 km because of the lack of seismic stations on the seafloor of the PO. The seismic ray takeoff angles proceed downward from the events to the seismic stations on land, and they do not pass through the shallow zone beneath the ocean since the distance from the hypocenter to the seismic stations is usually over 150 km. We investigated the 3D seismic velocity structure of and around Japanese Islands including the Sea of Japan and PO by the seismic tomographic method. We added the arrival time data detected in the S-net, the DONET, and the Hi-net datasets, operated by NIED, as well as other datasets, operated by multiple organizations, after 2016 in addition to the data used in [14]. Then we applied the seismic tomography to these datasets.

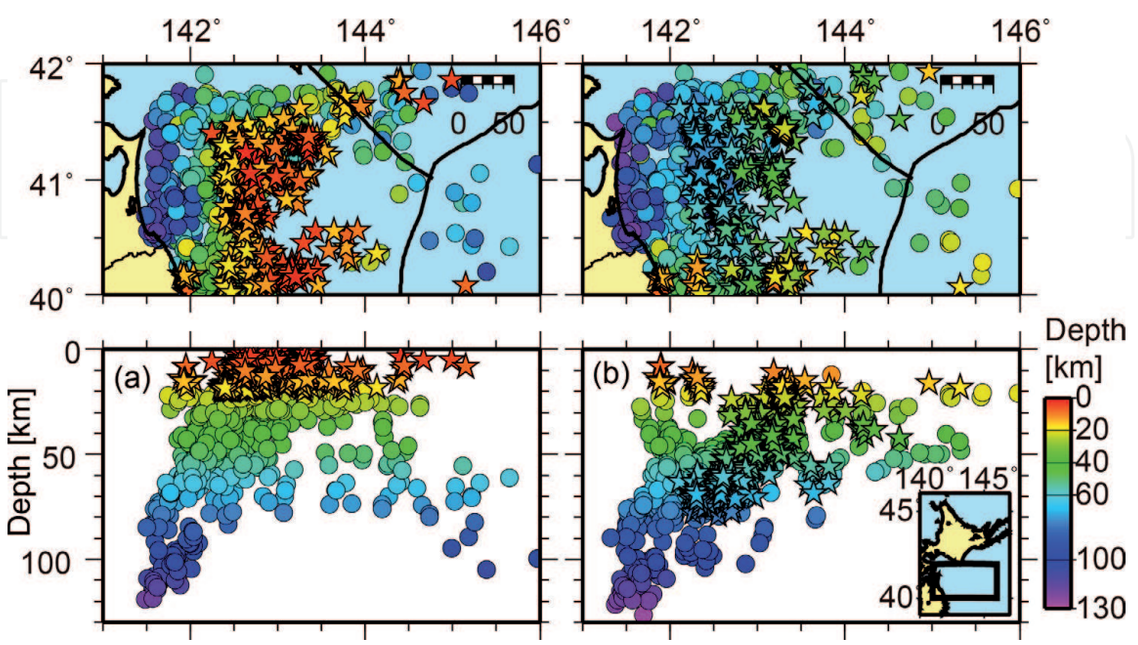

Figure 2.
Comparison of hypocenters determined by the NIED (a) Hi-net and (b) Hi-net and S-net. Stars denote hypocenters determined at depths shallower than 20 km by only Hi-net in (a) and redetermined by Hi-net and S-net in (b).

2. Data and method

The target region, 20–48°N and 120–148°E, covers the whole Japanese Islands from Hokkaido to Okinawa and the seismic stations both Hi-net on land and S-net and DONET beneath the ocean. In addition to the arrival time data used by [14], 1,782,425 P- and 1,528,733 S-wave arrival times from 32,952 earthquakes recorded at approximately 2000 stations including NIED S-net and DONET from April 2016 to June 2018 were selected. A total of 7,853,757 P-wave arrival data and 4,604,780 S-wave arrival data from 112,631 events are available after merging the new datasets (**Figure 3**).

We used the seismic tomographic method [15, 16] with spatial velocity correlation and station corrections to the original code by [11]. Grid nodes were placed with half of the spatial resolution. We performed smoothing in order to stabilize the solution for the inverse problem with the LSQR algorithm [17] since arbitrary damping matrix with combination of diagonal and smoothing matrices could be assumed.

We placed 3D grid nodes to construct the velocity (slowness) structure with the grid spacing shown in **Table 1** and adopted the 1D structure used in the routine determination of hypocenters at the Hi-net and S-net [18] as the initial velocity model (**Figure 4**). No velocity discontinuities such as Moho discontinuities or the plate boundary between the EUR and PAC or PHS plates were assumed in this study. This is because there were enough data to estimate the steep velocity gradient to represent plate boundaries so that velocity discontinues in the model were not necessary [13, 16, 19]. The total number of unknowns, 4,417,505, for P-wave slowness is the same as those for S-wave slowness. We solved the P- and S-wave slowness at each grid node from more than 10 associated rays.

First, we inverted the P- and S-wave seismic velocities using the initial hypocenter location. Second, both hypocenters and 3D seismic velocity structure were inverted simultaneously. We included the arrival times from the events beneath the ocean before 2015 in addition to the data used by [14]. Focal depths of offshore events were determined by NIED F-net or [20] since offshore events determined by only NIED Hi-net are not reliable. For these offshore events, only epicenters are inverted by the 3D seismic velocity structure, while hypocenter depths are fixed.

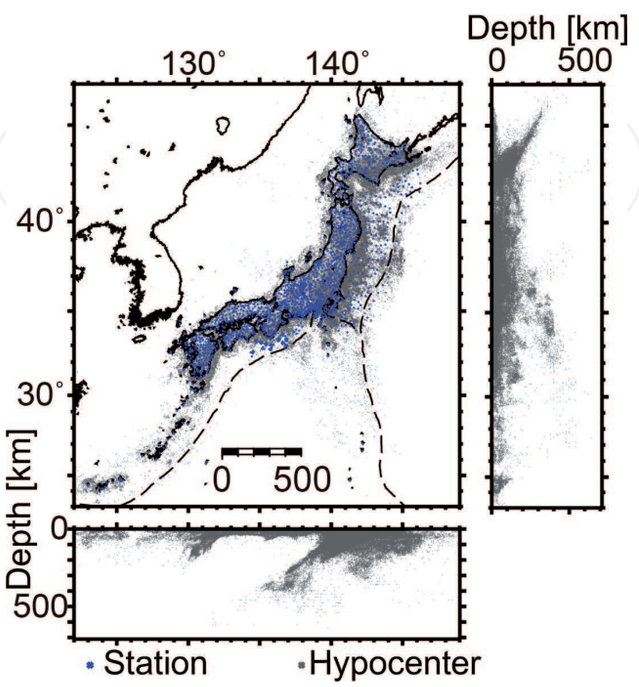

Figure 3.
Distribution of hypocenters and seismic stations used for seismic tomography.

Depth	Grid interval		Resolution/checkerboard pattern	
	Horizontal	Vertical (km)	Horizontal	Vertical (km)
0–10	0.1°	2.5	0.2°	5
10–40		5		10
40–60		10		20
60–180		15		30
180–300		20		40
300–		25		50

Table 1.
Grid interval and resolution size.

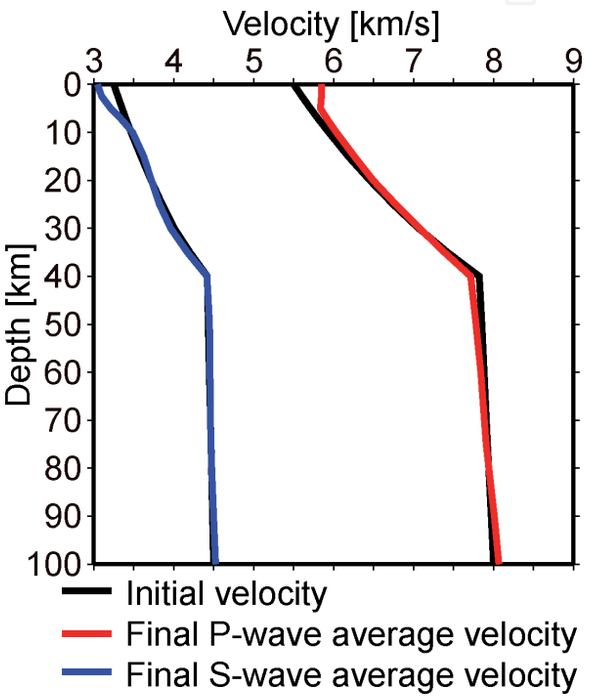

Figure 4.
Seismic velocity structures of the initial model and the average of the final 3D model.

We do not fix any condition for the events after 2016 detected by NIED S-net and DONET and the events within 50 km of the onshore seismic networks before 2015 during the inversion.

Residuals are improved to within 0.5 s for P-wave and 0.6 s for S-wave in the travel time inversion. In the final iteration, we used 6,356,481 P-wave arrival data and 3,534,482 S-wave arrival data to solve for the P-wave slowness at 1,135,165 grid nodes and the S-wave slowness at 1,103,525 grid nodes. The inversion reduces RMS of the P-wave travel time residual from 0.561 to 0.192 s and that of the S-wave data from 0.812 to 0.239 s after 11 iterations.

We conducted a checkerboard resolution test to evaluate the reliability of our solution [21]. We assumed a ± 5% checkerboard pattern and calculated synthetic travel times with random noise of 0 mean and standard deviations of 0.13 and 0.24 s for P- and S-waves, respectively. The standard deviations for random noise were derived from the average of the estimated uncertainty of the manually picked arrival times. The weight of data is inversely proportional to each width of picking error. The damping factors for the P-wave inversion are twice those for the S-wave inversion, since the average standard deviation of P-wave picking errors is almost half of that of S-wave.

3. Results

3.1 Results of checkerboard resolution test

Figure 5 shows the results of checkerboard resolution test. We calculate the recovery rate and stability with surrounding grid nodes in order to confirm well-resolved area [15]. The resolutions of Vp and Vs at depths of 5–30 km beneath main four islands are good. At depths of 40–60 km, resolutions are not good along the Sea of Japan coast because there are few deep earthquakes that can be used for inversion.

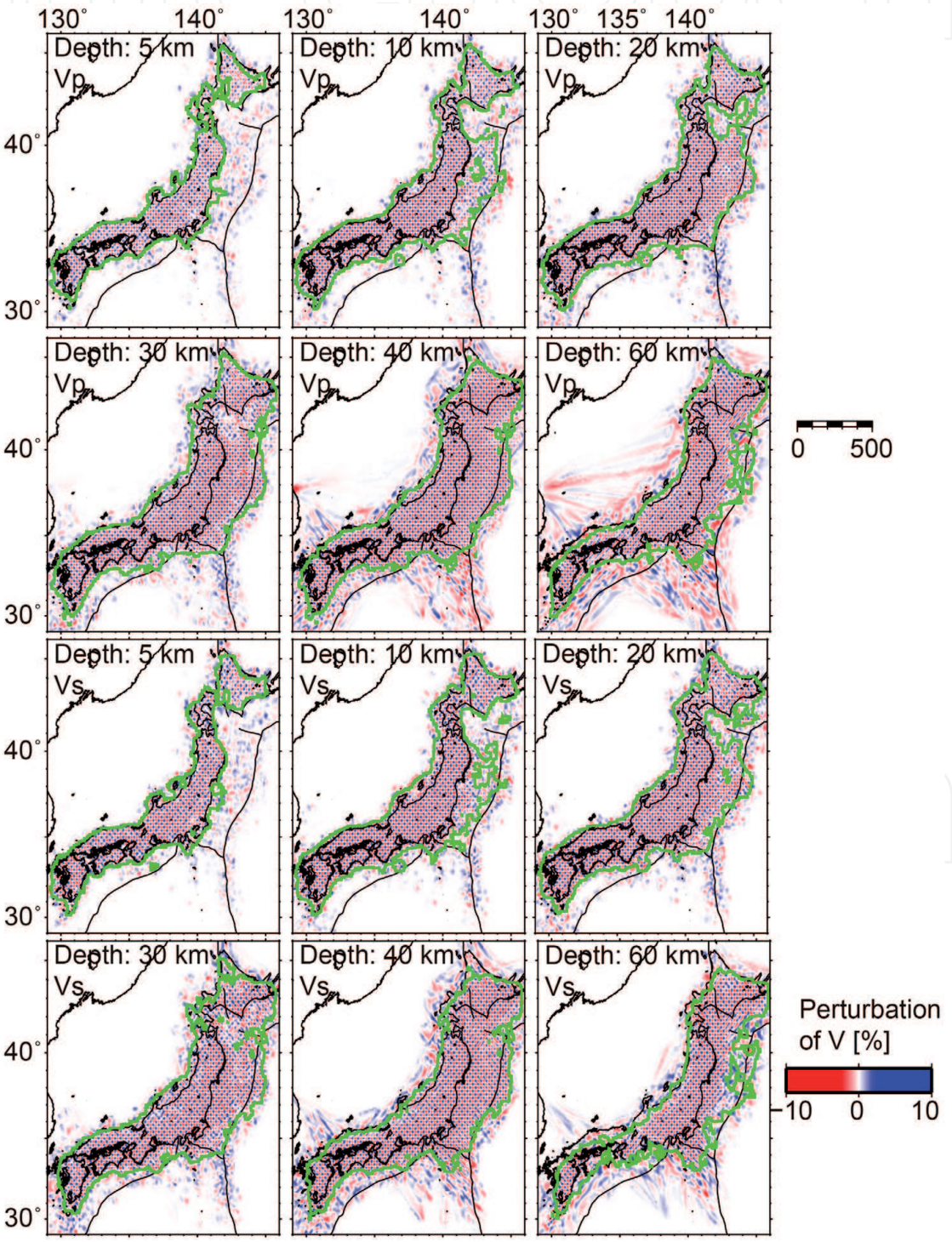

Figure 5.
Map views of checkerboard resolution test for Vp and Vs. green line surrounds the well-resolved area.

NIED S-net data increase the resolution at depths of 10–60 km from Honshu to the Japan Trench (**Figure 5**). Reference [14] used the offshore events such as aftershocks of the Tohoku-oki earthquake. The presence of a seismic station above the events is extremely important for the estimation of velocity structure as well as the determination of hypocenters. The resolutions at depths of 0 and 5 km are still not good in spite of the use of S-net data because the incident angle to the S-net stations are mainly steep and ray paths do not run horizontally because of the lack of shallow earthquakes. Resolutions near the triple junction of Japan Trench and Sagami Trough where three plates, PAC, PHS, and EUR, meet are good at depths of 20–30 km. This is an advantage of using NIED S-net.

Beneath the DONET area, the resolution at depths of 10–60 km is good for Vp, and those at depths of 5–40 km are good for Vs. The resolved zone extends to the Nankai Trough since there is sufficient seismicity in this area.

3.2 Map views at depths

We calculated the average 1D model from the final 3D velocity structure (**Figure 4**). We also showed the perturbation from these average velocities (**Figure 6**).

At a depth of 5 km, low-Vp and low-Vs regions are located along the PAC coast beneath southeastern Hokkaido, northeastern Honshu, most of Kanto, Sagami Bay, southern Kinki, and southern Shikoku regions. A low-Vs region extends beneath the entire Shikoku and southern Chugoku regions. A low-Vp/Vs region runs along the Ou backbone range in northeastern Japan and central Japan. Other regions have high Vp/Vs.

At a depth of 10 km, low-Vp regions extend beneath the active volcanoes in the northeastern and central Honshu and Kyushu regions. Low-Vs regions are almost the same as those at a depth of 5 km. High-Vp/Vs regions are distributed at central Hokkaido and coastal area in northeastern Japan. Low-Vp/Vs covers the other regions.

At a depth of 20 km, low-Vp regions lie beneath volcanoes in Hokkaido, central Honshu, and Kyushu. Low-Vs regions extend beneath the volcanoes and back-arc side of Honshu. Both low-Vp and low-Vs regions extend from central Kinki to

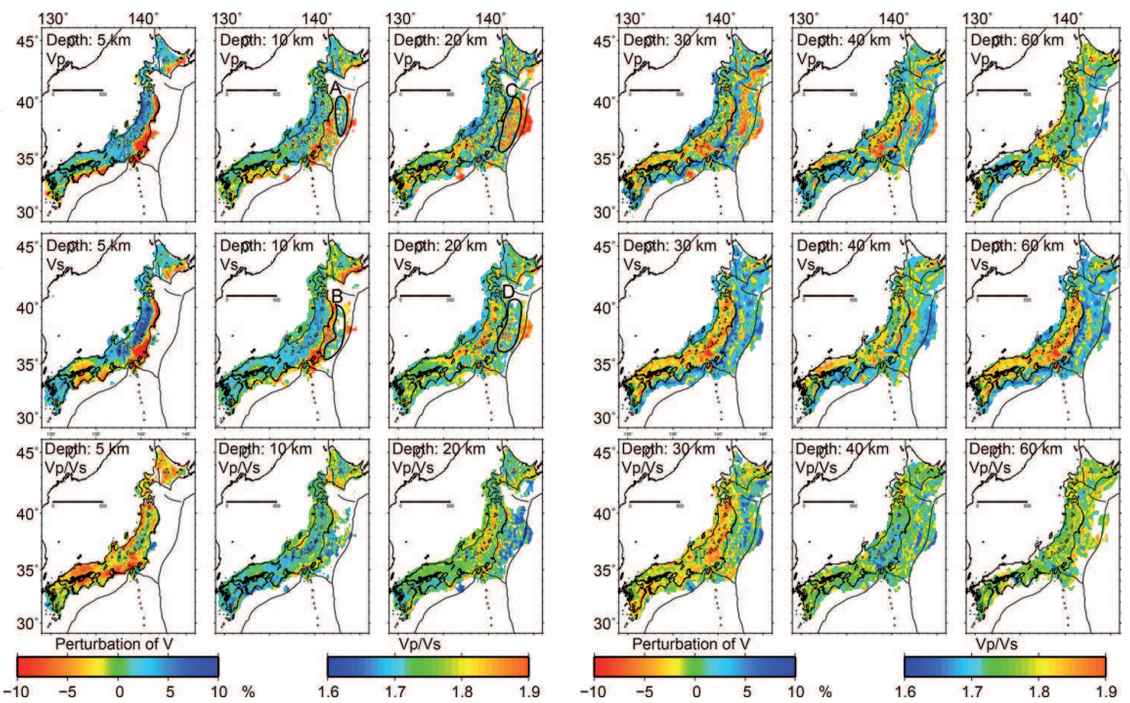

Figure 6.
Map views of Vp and Vs perturbation and Vp/Vs. Colored area is the resolved area. Broken white lines at depths of 10 and 20 km denote the median tectonic line.

Kyushu region across central Shikoku. This low-V zone remains the same as at a depth of 5 km. High-Vp/Vs regions cover the Ou backbone range and back-arc side of northeastern Honshu.

At a depth of 30 km, low-Vp extends beneath the northeastern Honshu, central and southwestern Honshu, and northern Kyushu regions. Low-Vs regions extend beneath most of Honshu, Kyushu, and northern Shikoku regions. High-Vp/Vs regions cover almost all Japanese Islands except the central Hokkaido.

At a depth of 40 km, low-Vp regions exist beneath the volcanoes in southeastern Hokkaido and northeastern and central Honshu regions. The low-Vp regions beneath the volcanoes in the northeastern Japan extend to back-arc side. Low-Vs regions are clarified beneath the volcanoes in southeastern Hokkaido and central Honshu regions. Low-Vs regions beneath the northeastern Honshu can be found east of the volcanic front as are low-Vp regions. Low-Vp/Vs regions cover the central mountains across Hokkaido and northeastern and central Honshu.

At a depth of 60 km, low-Vp and low-Vs regions extend beneath the volcanoes in Honshu and central Honshu. High-Vp and Vs regions extend beneath the Kinki, Shikoku, and eastern Kyushu regions where the PHS plates subduct. High-Vp/Vs regions are distributed across western Hokkaido, central Honshu, and central Shikoku regions.

At a depth of 90 km, low-Vp and low-Vs regions exist beneath the volcanoes beneath Hokkaido and Honshu. High-Vp and Vs regions extend to the east of northeastern Japan where the PAC plate subducts. High-Vp/Vs regions cover northern and southwestern Hokkaido, central Honshu, and central Kyushu regions.

3.3 Velocity structure beneath the Pacific Ocean off northeastern Japan beneath the S-net

At a depth of 10 km, a low-Vp and low-Vs zone extends along the coast of the PO in the northeastern Honshu. A high-Vp and high-Vs zone exists between the longitudes of 142 and 143°. East of longitude of 143° (**Figure 6A** and **B**), low-Vp, and low-Vs zone shows again. Vp/Vs is generally low except in some small regions.

At a depth of 20 km, a high-Vp and high-Vs zone extends along the coast of the PO in the northeastern Honshu, in contrast to the structure at a depth of 10 km. Low-V zones extend to the east of the high-Vp zone; however, some high-Vp zones exist among the low-Vp zones (**Figure 6C**). High-Vs zones are mixed with minor low-Vs zone off the east of northeastern Honshu, extending to a longitude of 143.5° (**Figure 6D**). This pattern can be seen with Vp at a depth of 10 km. Vp/Vs is also broadly low, and this pattern of Vp/Vs can be seen when the depth is 10 km except in some regions.

At a depth of 30 km, low-Vp zone extends off the east of northeastern Honshu between longitudes of 142 and 143.5 and to the region off the southeast of Hokkaido. High-Vp zone can be seen along the Japan Trench. Two patches of low-Vs zones exist in the east of northeastern Honshu at latitude of 37–40° and longitude of 142–143° and at latitude of 35–36° and longitude of 141–142°. High-Vp/Vs region is bounded by the low-Vp/Vs region, a north–south "stripe" pattern.

At a depth of 40 km, low-Vp and low-Vs zones extend between longitude of 142–143° and latitudes of 37–41°. These low-Vp and low-Vs zones extend to the west of the Hidaka Mountains. High-Vp and high-Vs zones can be seen on the east of the low-V zone and reach the east of the Japan Trench. Vp/Vs in this area is moderate except for some low-Vp/Vs regions with north–south trend.

At a depth of 60 km, low-Vp and low-Vs zones extend just off the coast of the PAC in the northeastern Honshu. High-Vp and high-Vs zones extend broadly on the east of the narrow low-V zone. Vp/Vs in this area is high.

3.4 Velocity structure beneath the Pacific Ocean off Kii and Muroto peninsula beneath the DONET

At depths of 20 and 30 km, low-Vp zones extend around the hypocenters of the large events with magnitude 6.9 and 7.4 that occurred on September 5, 2004. Low-Vs zones partly exist within the low-Vp zone. We cannot resolve the continuous structure from Honshu at depths of 5–10 km since the number of events for seismic tomography beneath the DONET stations is small. This is because the DONET picked data are basically added after the Hi-net manual picking. The seismic tomography will be recalculated when the microearthquake data triggered at DONET stations become available.

3.5 Station corrections

The station corrections for the final model are shown in **Figure 7**. Red stations denote positive O-C travel times. It means that the modeled velocity is too high due to thick sediment or low-V materials since the calculated travel time is too small. It also depends on the depth of borehole of Hi-net stations. The seismometers of the Hi-net stations are typically deployed at depths of around 100–200 m, and low-Vp sediment materials are estimated beneath the backbone range and back-arc side of Japan. Large station corrections are estimated along the Sea of Japan coast in northeastern Honshu since there are thick sediments, while borehole stations are relatively shallow. For Vs, there are many blue-colored stations meaning that the velocity model is too slow. Large station corrections are also estimated on the Sea of Japan side of northeastern Honshu.

For S-net stations, blue stations can be seen near the coast and the Japan Trench. Red stations are shown between them for both Vp and Vs. It suggests that the seismic velocity model is too slow near the coast and the Japan Trench and too fast between them.

For DONET stations, red stations are shown near the coast and blue stations reside off the coast. It means that the modeled seismic velocity is too high near the coast.

3.6 Movement of hypocenters

Figure 8 shows the histogram of the epicentral movement during the iterations. Epicenters determined by NIED F-net and [20] are shifted over 50 km

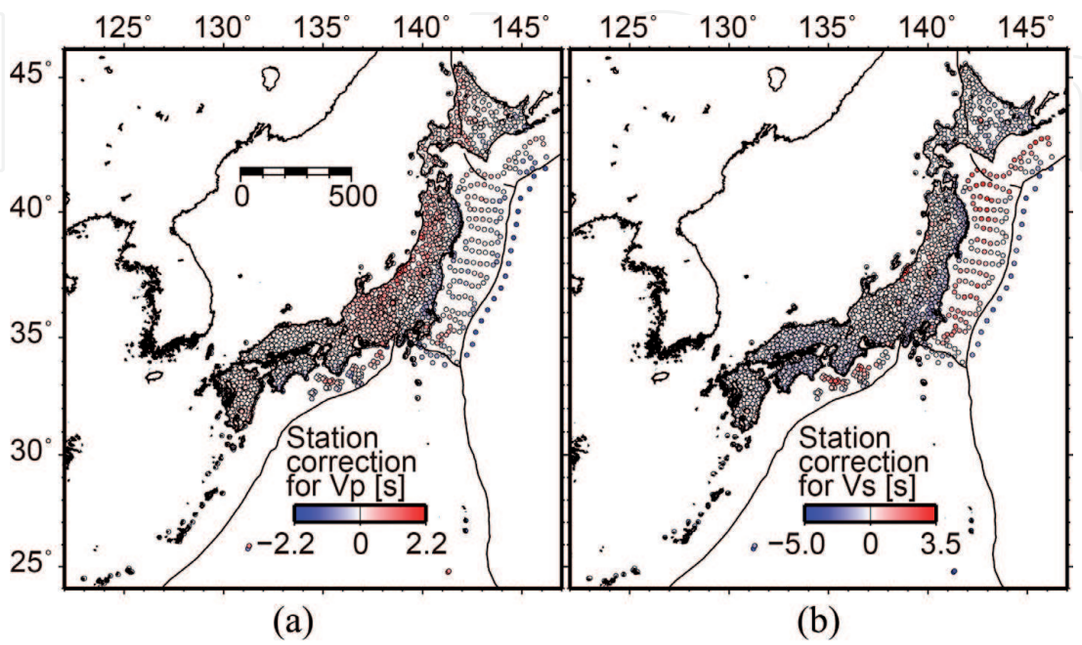

Figure 7.
Station corrections for (a) Vp and (b) Vs.

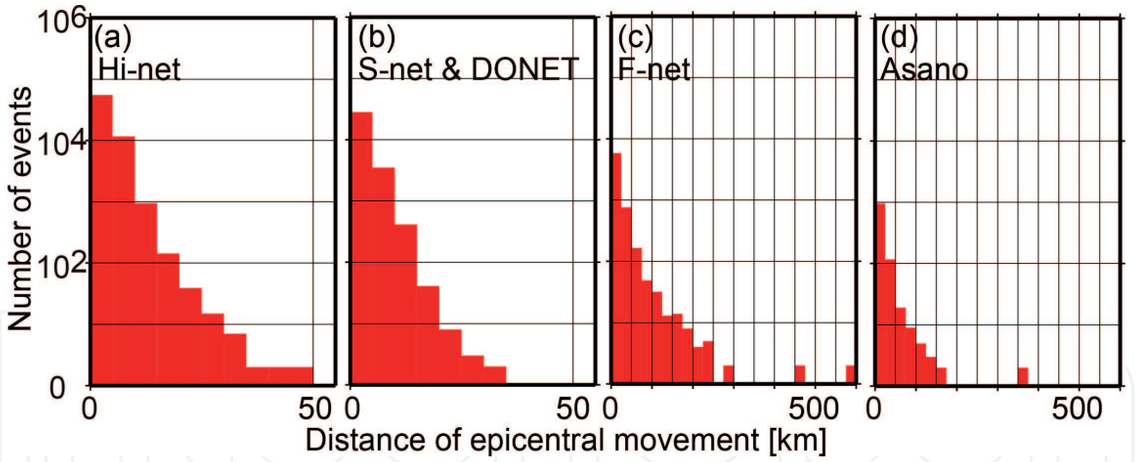

Figure 8.
Histogram of the earthquake epicentral movements during the inversion. The initial epicenters are determined by (a) NIED Hi-net; (b) NIED Hi-net, S-net, and DONET; (c) NIED F-net; and (d) Ref. [20]. The Hi-net system also uses the seismic stations operated by the other organizations.

after the inversion. Epicenters determined by NIED Hi-net or by NIED Hi-net, S-net, and DONET are mainly less than 10 km in spite of 11 iterations of inversion.

4. Discussion

4.1 Expanded resolved zone from the previous studies

Ref. [14] also clarified the seismic velocity structure beneath the PO at depths of 30–50 km; however, that study could not resolve the shallow structure at depths of 0–20 km since the ray paths, such as head waves, from the oceanic event to the land seismic stations pass through the deep zone. The ray paths from the events to NIED S-net stations run through the shallow part of the PO. In this study, we can clarify the structure at depths of 10–60 km and even east of the Japan Trench at depths of 20–30 km (**Figures 5** and **6**). This is a major improvement enabled by including NIED S-net data

4.2 Characteristic structure of the NS trending high-V and low-V zone off the northeastern Japan

One important feature is the probable Mesozoic rift structure trending NS from the coast of Tohoku to the west of Hidaka Collision Zone. The recent 2018 Hokkaido Eastern Iburi earthquake (M6.7) (Iburi earthquake) occurred at a depth of around 32 km, which is much deeper than the usual inland crustal earthquake. Unfortunately, the structure beneath the PO between the Honshu and Hokkaido islands at a depth of 20 km is not clear; however, a low-Vp zone at a depth of 30 km in north–south direction between 142 and 143° (**Figure 9**) is resolved. Low-Vp zones also exist west of the Hidaka Mountains and between the Honshu and Hokkaido at the northern extension of this low-V zone, although the high-Vp zone parallel to the Japan Trench along the coast of Honshu and Hokkaido invades the low-Vp zone. The high-Vp zone is consistent with the large positive Bouguer gravity anomaly [22] and large positive aeromagnetic anomaly zones [23]. It implies that high-V mantle mafic material is located in the shallow zone. The depth of the Moho is also shallow near the coast of northern Honshu [24]. The Iburi earthquake may be

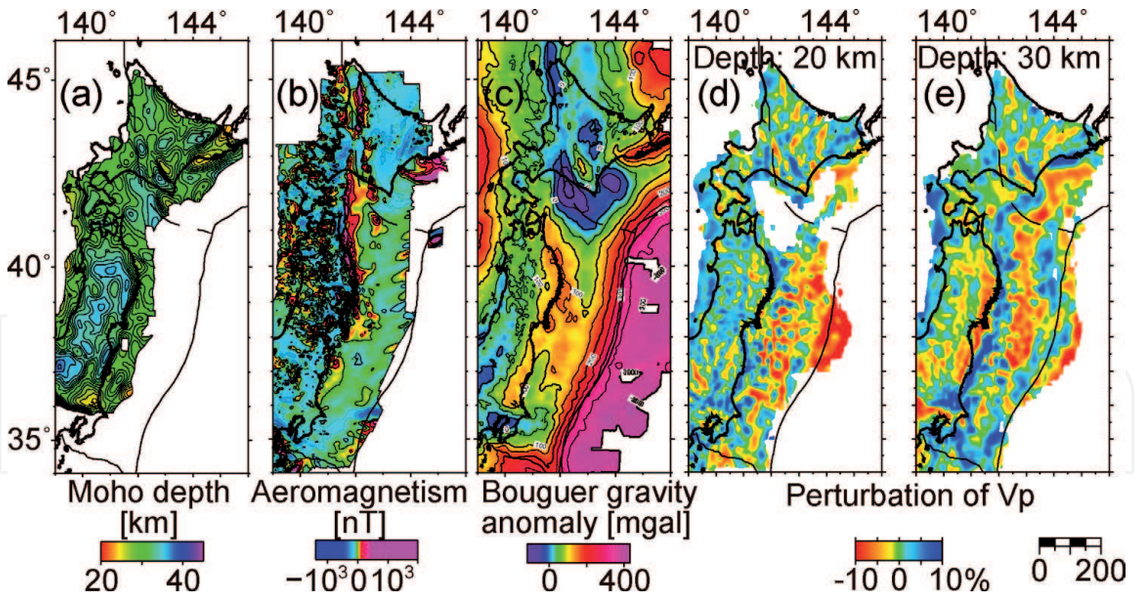

Figure 9.
Map views of (a) Moho depth, (b) aeromagnetism, (c) Bouguer gravity anomaly, Vp perturbation at depths of (d) 20 km and (e) 30 km beneath northern Japan.

related to the reactivation of the rift related to the structure in the upper mantle to the lower crust, where it is marked by high-Vp.

4.3 Characteristic structure along the sea of Japan

We clarified the seismic velocity structure beneath the Sea of Japan at depths of 10–20 km from offshore Hokkaido to Wakasa Bay (**Figure 6**). The Vp beneath the Okushiri and Sado Islands is low at a depth of 10 km; however, Vp beneath the Sea of Japan is high at depths of 10–35 km. Vp along the coast of Sea of Japan in western Japan gives moderate value. The lithospheric velocity structure in this region is strongly affected by the Mid-Tertiary breakup and formation of the Sea of Japan. Through the reactivation of the younger compressed tectonic terrain, tsunamigenic source faults have been developed. The lithospheric structure provides essential information to infer the structure of faults.

4.4 Comparison with the structure obtained by the offshore experiments

Ref. [25] imaged the bending-shaped low-Vp oceanic crust of PAC plate subducting from the Japan Trench at latitudes of 38–38.5° offshore Miyagi where the rupture of large interplate earthquakes propagated. In this study, low-Vp material is imaged at depths of 40–50 km bounded by the high-Vp materials with a number of earthquakes surrounded with red ellipse in **Figure 10**. It indicates the subducting oceanic crust of the PAC plate

The isovelocity contour of Vp = 7.0 km/s lies around depths of 25–40 km. Active-source seismic experiments off Sanriku region imaged the same contour lying at depths of 20–35 km [25] on the west side of Japan Trench, at depths of 15–30 km at the Japan Trench [26], and at depths of 15–25 km in NS direction between Honshu and Japan Trench [27]. The seismic velocity model of this study is relatively slower than those models derived from seismic experiments. The difference may depend on the initial velocity model of the oceanic region being set as the same as the land area in this study. The Moho depth becomes shallower with the EUR crust toward the Japan Trench. The oceanic crust of the PAC plate has also thinner crust than the EUR island arc crust.

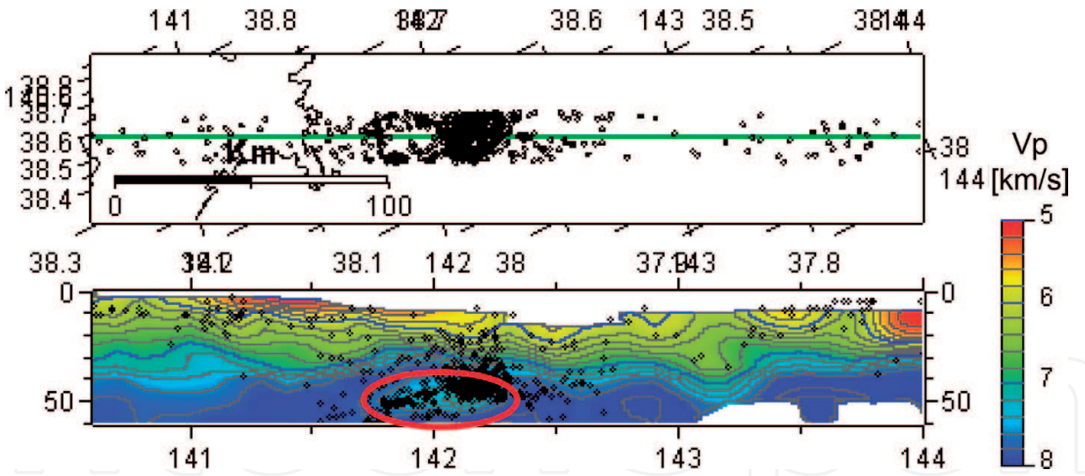

Figure 10.
Vertical cross section beneath the Pacific Ocean off Miyagi in WNW-ESE direction. Black circle shows the relocated hypocenters used for seismic tomography in this study.

4.5 Comparison of velocity structure on the coseismic slip plane of the Tohoku-oki event

Figure 11 shows the Vp perturbation just above the upper boundary of the PAC plate within the overriding EUR plate. The plane with the upper side at surface has a dip angle of 15°. Reference [28] also showed the Vp perturbation [29] above the upper boundary of the subducting PAC slab and three low-V zone offshore Sanriku, Miyagi, and Ibaraki. In our results, we obtain velocity structure in fine scale; however, we do not estimate the shallow structure along the Japan Trench. We obtain the broad low-Vp and low-Vp/Vs zone within the overriding EUR plate between the Japan Trench and Honshu. A high-Vp and slightly high-Vp/Vs zone exists on the

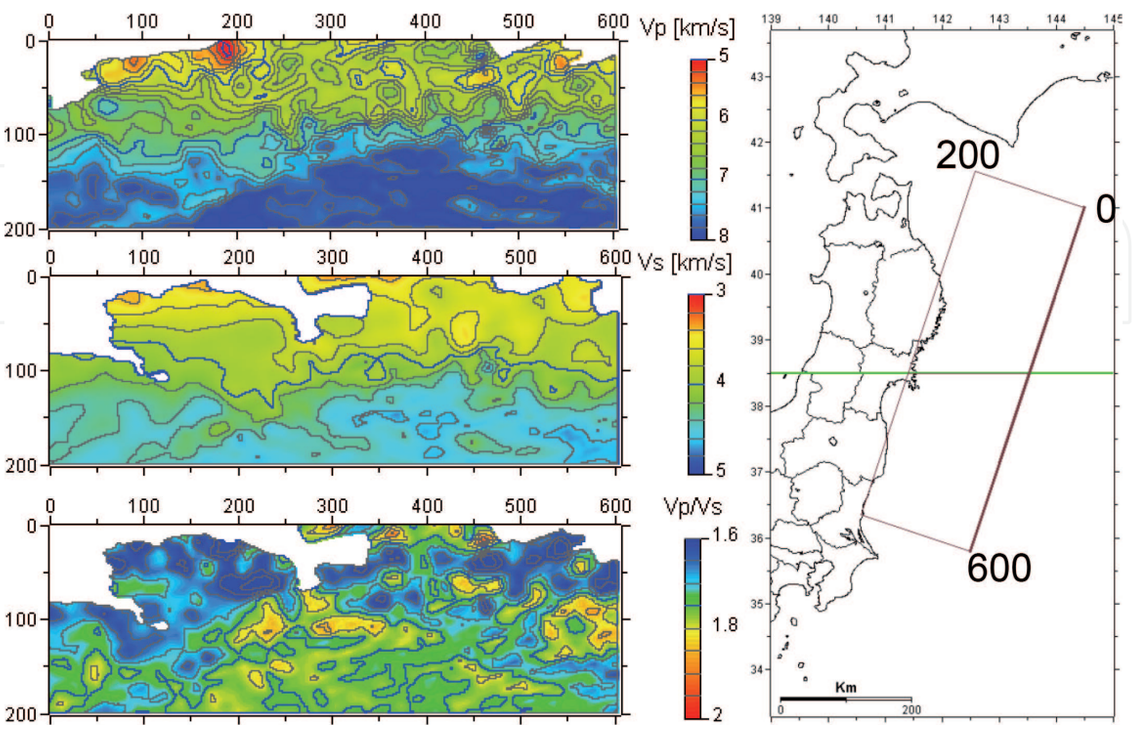

Figure 11.
Vp perturbation on the plane just above the upper boundary of the PAC plate within the overriding EUR plate. The plane has strike with S17degW from the point with a longitude of 144.5 and a latitude of 41.0 with dip angle of 12 deg. The depth of the upper edge of the plane is 10 km.

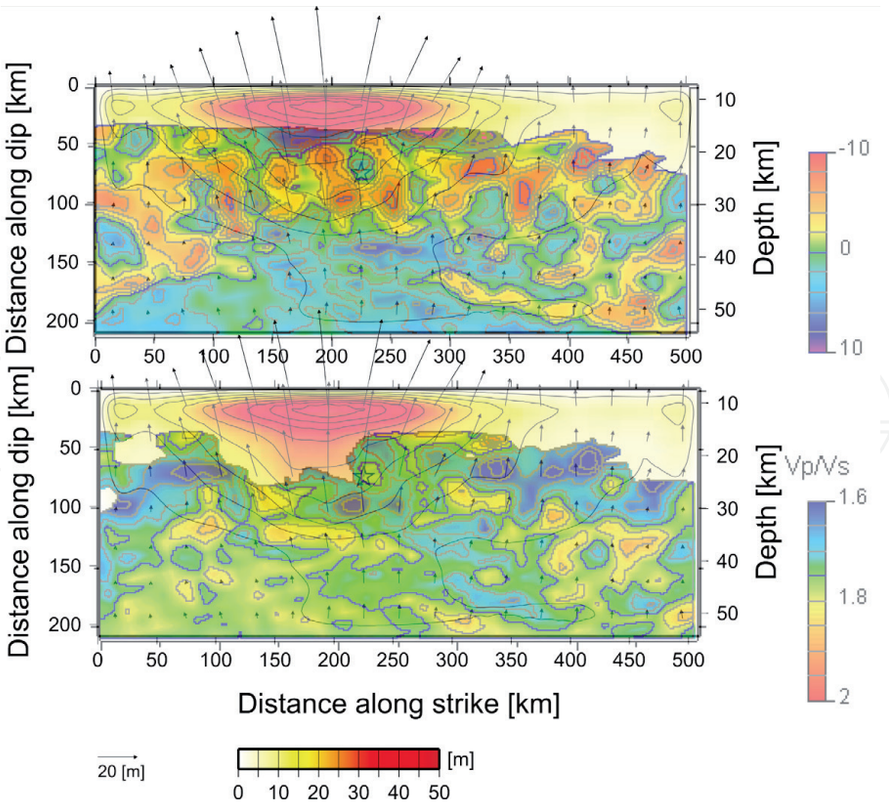

Figure 12.
(a) Vp perturbation and (b) Vp/Vs on the coseismic slip plane [30].

west side of the low-Vp and low-Vp/Vs zone. There are some small high-V zones within the low-V zone near the hypocenter of the Tohoku-oki event.

Figure 12 also shows the Vp perturbation and Vp/Vs on the coseismic plane of the Tohoku-oki event [30]. We do not obtain the shallow structure along the Japan Trench although the extremely large slip of the Tohoku-oki event is estimated near the Japan Trench. The western edge of the large slip zone is consistent with the high-Vp zone; however, the surrounding region has low-Vp and low-Vp/Vs. Low-Vp/Vs material is difficult to deform so that it can generate large elastic waves if it fails. Low-Vp/Vs on the coseismic slip region may be one of the reasons for the extreme size of the Tohoku-oki event.

5. Conclusion

We conducted the seismic tomography for entire Japanese Islands including oceanic area. This is the first tomographic study to use the data from NIED S-net. The hypocenters of oceanic events are greatly improved using the S-net data. We also obtain the detailed seismic velocity structure beneath the PO at depths of 10–60 km. Low-Vp and low-Vs zones are revealed between 142 and 143° at a depth of 30 km and in western Hokkaido where the Eastern Iburi Earthquake in 2018 occurred. The lithospheric velocity structure on the coast of Sea of Japan on Honshu is strongly affected by the Mid-Tertiary breakup and formation of the Sea of Japan. Tsunamigenic source faults have been developed through the reactivation of the younger compression. Subducting low-V oceanic crust is imaged within the mantle of overriding EUR and subducting oceanic PAC plate. The coseismic slip plane of the Tohoku-oki event has low-Vp/Vs; however, the shallow structure along the Japan Trench will be improved in the future with increased data. Previous seismic reflection and refraction studies found the oceanic crust at the uppermost part of the PAC

plate with Vp of approximately 6–7 km/s; however, the seismic tomography with NIED S-net clarified the 6–7 km/s Vp zone at depths of 25–40 km. The result may depend on the initial velocity model beneath the PO, which was the same initial model as the land area in this study. Applying the initial velocity model derived from the refraction or reflection seismology would improve the results beneath the ocean in the future.

Acknowledgements

We used the seismic data provided by the National Research Institute for Earth Science and Disaster Resilience, the Japan Meteorological Agency, Hokkaido University, Hirosaki University, Tohoku University, the University of Tokyo, Nagoya University, Kyoto University, Kochi University, Kyushu University, Kagoshima University, the National Institute of Advanced Industrial Science and Technology, the Geographical Survey Institute, Tokyo Metropolis, Shizuoka Prefecture, Hot Springs Research Institute of Kanagawa Prefecture, Yokohama City, and Japan Agency for Marine-Earth Science and Technology. This study was supported by the project on the Operation of Seismograph Networks for NIED. We thank academic editor Masaki Kanao for checking and commenting on our manuscript. We also thank David Shelly and Tomoko E. Yano for their helpful comments and improvement of our manuscript. Some of the figures were drawn using Generic Mapping Tools software [31] and the software for viewing 3D velocity structures beneath whole Japan Islands [32]. This work was financially supported in part by Japanese Ministry of Education, Culture, Sports, Science and Technology (MEXT) and by the Council for Science, Technology and Innovation (CSTI) through the Cross-ministerial Strategic Innovation Promotion Program (SIP), entitled "Enhancement of societal resiliency against natural disasters" (Funding agency: Japan Science Technology Agency).

Author details

Makoto Matsubara[1*], Hiroshi Sato[2], Kenji Uehira[1], Masashi Mochizuki[3], Toshihiko Kanazawa[4], Narumi Takahashi[1], Kensuke Suzuki[5] and Shin'ichiro Kamiya[1]

1 National Research Institute for Earth Science and Disaster Resilience, Tsukuba, Japan

2 Earthquake Research Institute, The University of Tokyo, Bunkyo, Japan

3 Ministry of Education, Culture, Sports, Science and Technology, Chiyoda, Japan

4 Association for the Development of Earthquake Prediction, Chiyoda, Japan

5 Japan Agency for Marine-Earth Science and Technology, Yokohama, Japan

*Address all correspondence to: mkmatsu@bosai.go.jp

References

[1] National Research Institute for Earth Science and Disaster Resilience, NIED Hi-net, National Research Institute for Earth Science and Disaster Resilience. DOI: 10.17598/NIED.0003

[2] Obara K, Kasahara K, Hori S, Okada Y. A densely distributed high-sensitivity seismograph network in Japan: Hi-net by National Research Institute for Earth Science and Disaster Prevention. Review of Scientific Instruments. 2005;**76**:021301. DOI: 10.1063/1.1854197

[3] National Research Institute for Earth Science and Disaster Resilience, NIED F-net, National Research Institute for Earth Science and Disaster Resilience. DOI: 10.17598/NIED.0005

[4] Okada Y, Kasahara K, Hori S, Obara K, Sekiguchi S, Fujiwara H, et al. Recent progress of seismic observation networks in Japan-Hi-net, F-net, K-NET and KiK-NET. Research News Earth Planets Space. 2004;**56**:xv-xxviii

[5] National Research Institute for Earth Science and Disaster Resilience, NIED DONET, National Research Institute for Earth Science and Disaster Resilience. DOI: 10.17598/NIED.0008

[6] National Research Institute for Earth Science and Disaster Resilience, NIED S-net, National Research Institute for Earth Science and Disaster Resilience. DOI: 10.17598/NIED.0007

[7] Kanazawa T. Japan trench earthquake and tsunami monitoring network of cable-linked 150 ocean bottom observatories and its impact to earth disaster science. In: IEEE International Underwater Technology Symposium (UT). IEEE; 2013. pp. 1, 2013-5

[8] Uehira K, Kanazawa T, Mochizuki M, Fujimoto H, Noguchi S, Shinbo T, et al. Outline of seafloor observation network for earthquakes and tsunamis along the Japna trench (S-net). EGU General Assembly. 2016;**2016**:EGU2016-EG13832

[9] National Research Institute for Earth Science and Disaster Resilience, NIED K-NET, KiK-net, National Research Institute for Earth Science and Disaster Resilience. DOI: 10.17598/NIED.0004

[10] National Research Institute for Earth Science and Disaster Resilience, NIED V-net, National Research Institute for Earth Science and Disaster Resilience. DOI: 10.17598/NIED.0006

[11] Zhao D, Hasegawa A, Horiuchi S. Tomographic imaging of P and S wave velocity structure beneath northeastern Japan. Journal of Geophysical Research. 1992;**97**:19,909-19,928

[12] Matsubara M, Obara K, Kasahara K. Three-dimensional P- and S-wave velocity structures beneath the Japan Islands obtained by high-density seismic stations by seismic tomography. Tectonophysics. 2008;**454**:86-103. DOI: 10.1016/j.tecto.2008.04.016

[13] Matsubara M, Obara K. The 2011 off the Pacific coast of Tohoku earthquake related to a strong velocity gradient with the Pacific plate. Earth, Planets and Space. 2011;**63**:663-667

[14] Matsubara M, Sato H, Uehira K, Mochizuki M, Kanazawa T. Three-dimensional seismic velocity structure beneath Japanese Islands and surroundings based on NIED seismic networks using both inland and offshore events. Journal of Disaster Research. 2017;**12**:844-857. DOI: 10.20965/jdr.2017.p0844

[15] Matsubara M, Hirata N, Sato H, Sakai S. Lower crustal fluid distribution in the northeastern Japan arc revealed by

high resolution 3D seismic tomography. Tectonophysics. 2004;**388**:33-45. DOI: 10.1016/j.tecto.2004.07.046

[16] Matsubara M, Hayashi H, Obara K, Kasahara K. Low-velocity oceanic crust at the top of the Philippine Sea and Pacific plates beneath the Kanto region, Central Japan, imaged by seismic tomography. Journal of Geophysical Research. 2005;**110**:B12304. DOI: 10.1029/2005JB003673

[17] Nolet G. Seismic Tomography. D. Reidel Publishing Company; 1987. p. 386

[18] Ukawa M, Ishida M, Matsumura S, Kasahara K. Hypocenter determination method of the Kanto-Tokai observational network for microearthquakes (in Japanese with English abstract). Research Notes National Research Center Disaster Prevention. 1984;**53**:1-88

[19] Matsubara M, Obara K, Kasahara K. High-Vp/vs zone accompanying non-volcanic tremors and slow slip events beneath southwestern Japan. Tectonophysics. 2009;**472**:6-17. DOI: 10.1016/j.tecto.2008.06.013

[20] Asano Y, Saito T, Ito Y, Shiomi K, Hirose H, Matsumoto T, et al. Spatial distribution and focal mechanisms of aftershocks of the 2011 off the Pacific coast of Tohoku earthquake. Earth, Planets and Space. 2011;**63**:669-673. DOI: 10.5047/eps.2011.05.018

[21] Inoue H, Fukao Y, Tanabe K, Ogata Y. Whole mantle P-wave travel time tomography. Physics of the Earth and Planetary Interiors. 1990;**59**:294-328

[22] Geological Survey of Japan. Gravity Database of Japan. DVD edition, Digital Geoscience Map P-2. Geological Survey of Japan, AIST. 2013

[23] Nakatsuka T, Okuma S. Aeromagnetic Anomalies Database of Japan. Digital Geoscience Map P-6. Geological Survey of Japan. 2005

[24] Matsubara M, Sato H, Ishiyama T, Van Horne AD. Configuration of the Moho discontinuity beneath the Japanese Islands derived from three-dimensional seismic tomography. Tectonophysics. 2017;**710-711**:97-107. DOI: 10.1016/j.tecto.2016.11.025

[25] Ito A, Fujie G, Miura S, Kodaira S, Kaneda Y, Hino R. Bending of the subducting oceanic plate and its implication for rupture propagation of large interplate earthquakes off Miyagi, Japan, in the Japan trench subduction zone. Geophysical Research Letters. 2005;**32**:L05310. DOI: 10.1029/2004GL022307

[26] Obana K, Fujie G, Takahashi T, Yamamoto Y, Tonegawa T, Miura S, et al. Seismic velocity structure and its implications for oceanic mantle hydration in the trench-outer rise of the Japan trench. Geophysical Journal International. 2019;**217**:1629-1642. DOI: 10.1093/gji/ggz099

[27] Fujie G, Kodaira S, Yamashita M, Sato T, Takahashi T, Takahashi N. Systematic changes in the incoming plate structure at the Kuril trench. Geophysical Research Letters. 2012;**40**:88-93. DOI: 10.1029/2012GL054340

[28] Zhao D, Huang Z, Umino N, Hasegawa A, Kanamori H. Structural heterogeneity in the megathrust zone and mechanism of the 2011 Tohoku-oki earthquake (Mw 9.0). Geophysical Research Letters. 2011;**38**:L17308. DOI: 10.1029/2011GL048408

[29] Huang Z, Zhao D. Mechanism of the 2011 Tohoku-oki earthquake (Mw 9.0) and tsunami: Insight from seismic tomography. Journal of Asian Earth Sciences. 2013;**70-71**:160-168

[30] Suzuki W, Aoi S, Sekiguchi H, Kunugi T. Rupture process of the 2011 Tohoku-Oki mega-thrust earthquake (M9.0) inverted from strong-motion data. Geophysical Research Letters. 2011;**38**:L00G16. DOI: 10.1029/2011GL049136

[31] Wessel P, WHF S. New version of generic mapping tools released. EOS Transactions. 1995;**79**:329

[32] Matsubara M. Software for viewing 3D velocity structures beneath whole Japan Islands. Report of the National Research Institute for Earth Science and Disaster Prevention. 2010;**76**:1-9